



Article

Physoxia Influences Global and Gene-Specific Methylation in Pluripotent Stem Cells

Fatma Dogan ^{1,†} , Rakad M. Kh Aljumaily ^{2,†}, Mark Kitchen ¹ and Nicholas R. Forsyth ^{1,*} 

¹ The Guy Hilton Research Laboratories, School of Pharmacy and Bioengineering, Faculty of Medicine and Health Sciences, Keele University, Stoke on Trent ST4 7QB, UK; f.dogan@keele.ac.uk (F.D.); m.o.kitchen@keele.ac.uk (M.K.)

² Department of Biology, College of Science, University of Baghdad, Baghdad 17635, Iraq; rakad.aljumaily@sc.uobaghdad.edu.iq

* Correspondence: n.r.forsyth@keele.ac.uk

† These authors contributed equally to this work.

Abstract: Pluripotent stem cells (PSC) possess unlimited proliferation, self-renewal, and a differentiation capacity spanning all germ layers. Appropriate culture conditions are important for the maintenance of self-renewal, pluripotency, proliferation, differentiation, and epigenetic states. Oxygen concentrations vary across different human tissues depending on precise cell location and proximity to vascularisation. The bulk of PSC culture-based research is performed in a physiologically hyperoxic, air oxygen (21% O₂) environment, with numerous reports now detailing the impact of a physiologic normoxia (physoxia), low oxygen culture in the maintenance of stemness, survival, morphology, proliferation, differentiation potential, and epigenetic profiles. Epigenetic mechanisms affect multiple cellular characteristics including gene expression during development and cell-fate determination in differentiated cells. We hypothesized that epigenetic marks are responsive to a reduced oxygen microenvironment in PSCs and their differentiation progeny. Here, we evaluated the role of physoxia in PSC culture, the regulation of DNA methylation (5mC (5-methylcytosine) and 5hmC (5-hydroxymethylcytosine)), and the expression of regulatory enzyme DNMTs and TETs. Physoxia enhanced the functional profile of PSC including proliferation, metabolic activity, and stemness attributes. PSCs cultured in physoxia revealed the significant downregulation of DNMT3B, DNMT3L, TET1, and TET3 vs. air oxygen, accompanied by significantly reduced 5mC and 5hmC levels. The downregulation of DNMT3B was associated with an increase in its promoter methylation. Coupled with the above, we also noted decreased HIF1A but increased HIF2A expression in physoxia-cultured PSCs versus air oxygen. In conclusion, PSCs display oxygen-sensitive methylation patterns that correlate with the transcriptional and translational regulation of the de novo methylase DNMT3B.

Keywords: pluripotent stem cells; characterisation; epigenetic; methylation; hydroxymethylation; physiological oxygen; DNA methyltransferase



Citation: Dogan, F.; Aljumaily, R.M.K.; Kitchen, M.; Forsyth, N.R. Physoxia Influences Global and Gene-Specific Methylation in Pluripotent Stem Cells. *Int. J. Mol. Sci.* **2022**, *23*, 5854. <https://doi.org/10.3390/ijms23105854>

Academic Editor: Akira Nifuji

Received: 28 April 2022

Accepted: 17 May 2022

Published: 23 May 2022

Publisher's Note: MDPI stays neutral with regard to jurisdictional claims in published maps and institutional affiliations.



Copyright: © 2022 by the authors. Licensee MDPI, Basel, Switzerland. This article is an open access article distributed under the terms and conditions of the Creative Commons Attribution (CC BY) license (<https://creativecommons.org/licenses/by/4.0/>).

1. Introduction

Epigenetics play a key role in pluripotency determination in human pluripotent stem cells (hPSCs) [1]. A powerful laboratory tool, hPSC, is exploited as an in vitro model system to explore differentiation and epigenetic changes during development processes [2,3]. Human-induced pluripotent stem cells (hiPSCs) are an effective complementary aid for hESCs (embryonic stem cells) studies due to their matched properties, including self-renewal and differentiation into multiple cell lineages [4,5]. Further, both hESCs and hiPSCs have a key role to play as cell sources for regenerative medicine and drug screening research [6,7]. hPSCs display unique epigenetic patterning when compared to differentiated and somatic cells that may contribute to unravelling developmental processes reliant on appropriate gene expression [8,9].

Epigenetic mechanisms consist of DNA methylation, histone modifications, and non-coding RNAs. These can modify chromatin and genomic structures and affect gene expression without changing DNA sequence [10,11]. DNA methyltransferase enzymes (DNMTs) include DNMT1, DNMT3A, DNMT3B, and accessory protein DNMT3L, and establish and maintain DNA methylation patterns in mammals [12]. The structure, mechanism, and function of DNMTs are well defined. DNMT1 is predominantly involved in the maintenance of DNA methylation during cell division while DNMT3A and DNMT3B, which work in coordination with DNMT1, are responsible for de novo methylation, typically during early development in embryonic stem cells [13,14]. DNMT3A and DNMT3B expression is high in undifferentiated ESCs, down-regulated post-differentiation, and remains low in adult somatic tissues [15,16]. *DNMT3A* and *DNMT3B* knockout cells can differentiate into the three existing germ layers (ectoderm, endoderm, mesoderm) [16]. Further, early passage *DNMT3A* and *DNMT3B* knockout-mouse ESCs can initiate and proceed to terminally differentiated cardiomyocytes and hematopoietic cells where DNMT1 is essential for the maintenance of their differentiation potential [17,18]. The knockout of DNMT3A and DNMT3B in ESCs does not impact their replication potential but does so in differentiated progeny [18].

Oxygen is fundamental for cellular processes. hESCs are derived from preimplantation blastocysts that undergo routine physiological exposure to a 2–5% oxygen environment [19] but paradoxically, air oxygen remains the predominant culture condition. Physiological oxygen tensions promote the maintenance of key properties in embryonic and mesenchymal stem cells, are an essential component of the stem cell microenvironment, and act as signalling molecules in the regulation of stem cell development [20]. Physoxia promotes hESC expansion, clonogenicity, transcriptional (mRNA and miRNA) changes, translational changes, genomic stability, altered metabolic activity, migration, and differentiation features [21–25].

The methylation of genomic CpG islands is correlated to transcriptional silencing and is required for normal development and the differentiation of hESCs [26]. Key transcription factors (Nanog and Oct4/Pou5f1), which maintain stem cell features in ESCs, are unmethylated in undifferentiated stem cells, and become methylated as differentiation progresses [27]. Physiological oxygen (1%) promotes a significant reduction in global DNA methylation levels in human colorectal, melanoma, and neuroblastoma cancer cell lines [28,29]. Moreover, in neuroblastoma, this is accompanied by increased *TET1* transcription and elevated global 5hmC levels with the accumulation of 5hmC density at the hypoxia response genes [29]. Similarly, hMSC (human mesenchymal stem cell) isolation and continuous exposure to 2% O₂ resulted in a significant decrease in global 5mC and 5hmC levels, accompanied by a reduced expression of DNMT3B and HIF1A but increased expression of HIF2A [30]. TET1 and TET2 expression is reported as playing a key role in cell fate and differentiation potential in undifferentiated ESCs [31]. TET1 activity, for example, is regulated by physiological O₂ in embryogenesis and is specifically inhibited by low (1%) O₂ [32]. The downregulation of *TET1* is associated with decreased global 5hmC, both in undifferentiated and 3-days differentiated mESC in 1% O₂; in addition, silencing *TET1* increases the expression of pluripotency markers and inhibits the differentiation potential of mESCs [32]. Our previous observations detailed reductions in global 5mC, 5hmC levels and TET1 expression in hMSCs cultured in physoxia [30]. *DNMT1* and *DNMT3B* promoters both possess HIF1A binding sites, suggesting that oxygen levels can play a role in the regulation of *DNMT1* and *DNMT3B* expression via HIF1A transcription factor [33,34]. A prolonged exposure to low oxygen culture is reported to be associated with decreased HIF1A expression in hESCs [19]. Consistent with this report, decreased DNMT3B and HIF1A expression was observed after long term culture in 2% O₂ in hMSCs [30]. The effects of physoxia on DNA methylation in hPSCs and differentiated progeny have received little attention so far.

In this study, we report a significant decrease in global methylation (5mC and 5hmC) and DNMT3B/TET1 expression, which is consistent with increased promoter-specific

methylation patterns linked to physoxia culture in PSCs. hPSCs have a great potential to provide new research tools for clinical applications such as drug screening and cell replacement therapies. Understanding the methylation patterning associated with hPSCs differentiation in physiological settings is essential for the development of functionally relevant models.

2. Materials and Methods

2.1. Cell Culture

SHEF1 and SHEF2 were obtained from the laboratory stock (Guy Hilton Research Centre) and used under the approval of the UK Stem Cell Bank (UKSCB) [35]. The human-induced pluripotent stem cell line (iPSC) (ZK2012L) derived from human dermal fibroblasts was kindly provided by Professor Susan Kimber and Dr Zoher Kapacee, Faculty of Biology Medicine and Health, University of Manchester. PSCs were routinely cultured in an E8 medium (Life Technologies) with Essential 8 Supplement (1×) in culture vessels coated with 5 mg/mL vitronectin (Recombinant Human Protein; Life Technologies, London, UK). The spontaneous differentiation medium was Knockout DMEM, 10% FBS, 1% NEAA, 1% L-glutamine and β-mercaptoethanol. hPSCs were grown in vitronectin-coated culture plates for 48 h in an E8 medium before switching into a spontaneous differentiation medium. Confluent cells were passaged enzymatically using the 0.5 mM EDTA (Fisher Scientific, Loughborough, UK) and incubated for 3–5 min at 37 °C until cells began to detach. Then, cells were collected in pre-warmed media and centrifuged at 1000 rpm for 3 min. Next, the supernatant was removed, the pellet was re-suspended in fresh media, and seeded at a minimum split ratio of 1:2. Cells were maintained in three different oxygen settings; 21% air oxygen (21% AO), a fully defined 2% O₂ environment (workstation) (2% WKS), and a standard 2% O₂ incubator (2% PG), where samples were handled in a standard class II biological safety laminar flow cabinet. Media utilised in a 2% O₂ setting was deoxygenated to a 2% O₂ level prior to use, using the defined Hypoxycool (Baker Ruskinn, Bridgend, UK) cycle settings.

2.2. Metabolic Activity of hPSCs

PSCs were seeded into 96-well plates at a density of 1×10^4 cells/cm², incubated for 24 h, an MTT stock solution (15 μL) was added to 150 μL of culture media and they were further incubated for 4 h at 37 °C. Following incubation, a 125 μL aliquot was removed and 50 μL of Dimethyl sulfoxide (DMSO) was added, then they were again incubated for 45 min at 37 °C. For the Alamar blue assay (Fisher Scientific, Loughborough, UK), 1×10^4 cells/cm² cells were cultured in flat-bottom 96-well plates for 48 h. The medium was then removed and replaced with a 100 μL fresh E8 medium supplemented with 10 μL Alamar blue reagent and incubated for 4 h at 37 °C. After the final incubation steps, both assays were measured with a plate reader (BioTek, Synergy 2, Agilent, Cheshire, UK) at a 570 nm wavelength. Data are presented as a mean ± standard deviation (SD) of the three triplicate experiments.

2.3. Flow Cytometry

Cells were characterised using the hPSC imaging kit (Human Pluripotent Stem Cell Marker Antibody Panel kit, SC008, R&D system, Abingdon, UK) with the analysis performed on a flow cytometer (Beckman Coulter Cytomics FC 500). hPSCs were labelled with pluripotency markers (SSEA-4, TRA-1-60 and SSEA-1) and 5×10^5 cells were used for each experiment. After harvest, pellets were re-suspended in the flow cytometry buffer (PBS with 0.5% (*w/v*) BSA and 2 mM EDTA, (Fisher Scientific)). The percentage of positive events was determined via the gate exclusion of 99% of the control events. Flowing Software was used for data analysis.

2.4. DNA Methylation Analysis

The DNeasy Blood and Tissue kit (Qiagen, Manchester, UK) was used to extract genomic DNA isolation from hPSCs. The total 5mC levels within genomic DNA were measured with the MethylFlash™ Methylated DNA Quantification Kit (Epigentek, Farmingdale, NY, USA) using 100 ng of input DNA. Total 5hmC quantification was performed with the MethylFlash™ Hydroxymethylated DNA Quantification Kit (Epigentek, Farmingdale, NY, USA) using 200 ng of input DNA. Methylation levels for both assays were established by reading absorbance at A450 nm via a microplate reader (BioTek, Synergy 2, Agilent, Cheshire, UK) using program Gen5 1.10 for quantification via the provided standards.

2.5. Pyrosequencing

Bisulphite conversion of 500 ng input genomic DNA per sample was performed using EZ DNA Methylation-Gold™ Kit (Zymo Research, Orange, CA, USA). Primers specific for DNMT1, DNMT3A, DNMT3B, DNMT3L, TET1, TET2, and TET3 were designed via the PyroMark Q24 Software 2.0 (Qiagen, Manchester, UK). Primer sequences and product sizes are listed in Table S2 and were supplied by Biomers (Ulm, Germany). Converted DNA (2–4 µL) was used as a template in the PCR reactions and amplifications were performed with the GoTaq® G2 Flexi DNA Polymerase kit (Promega, Southampton, UK). The cycling parameters were one cycle of 95 °C for 5 min for initial denaturation followed by touch-down cycling for the first 14 cycles, where the temperature was reduced by 0.5 °C in each successive cycle. This was followed by 35 cycles of 95 °C for 45 s, annealing at 55–63 °C for 45 s, elongation at 72 °C for 30 s, and a final elongation step at 72 °C for 5 min. PCR amplification product quality was confirmed via 2% agarose gel electrophoresis. Biotin-labelled PCR amplicons were captured by mixing PCR products with streptavidin-sepharose beads (GE Healthcare). The Vacuum Prep Tool with filter probes was used to capture sepharose beads with biotin-labelled PCR amplicons. Filter probes were washed with a 70% ethanol solution, then with a denaturation solution (NaOH) to denature PCR product and a washing buffer to purify the final biotinylated strands. The filter probes were carefully placed into the Q24 pyrosequencing plate wells and the beads were released into an annealing mix. Then, the pyroMark Gold Q24 Reagents, including the four nucleotides, the substrate and enzyme mix were loaded into a pyrosequencing dispensation cartridge. Pyrosequencing was started after the cartridge and Q24 pyrosequencing plate were inserted into the pyrosequencing instrument. Data were analysed using the PyroMark Q24 Software 2.0 (Qiagen, Manchester, UK).

2.6. Gene Expression

RNA was isolated from hPSCs with the RNeasy® Mini Kit (Qiagen, Manchester, UK) and the concentration was quantified using a NanoDrop™ 2000/2000c Spectrophotometer (Thermo Scientific, Waltham, MA, USA). RT-PCR was performed using the QuantiFast SYBR Green OneStep RT-PCR kit (Qiagen, Manchester, UK). PCR primers were obtained from Invitrogen Ltd. and ThermoFisher-Scientific (London, UK). The primer sequences and product sizes are listed in Table S1. PCR amplification was performed on 25 ng of isolated RNA and the relative quantification of gene expression was measured using the $2^{-\Delta\Delta CT}$ method. All primers had a 55 °C annealing temperature except DNMT3A at 56 °C.

2.7. DNMT3B Activity

The EpiQuik™ DNA Methyltransferase 3B Activity/Inhibitors Assay Core Kit (Insight Biotechnology, Wembley, UK) was used to analyse DNMT3B activity.

Blank control wells were labelled, then 3 µL (10 µg) samples were added to the appropriate wells. After samples were prepared, 27 µL of the DNMT Assay Buffer and 3 µL of diluted Adomet were added, 8 mM was added to each well, and they were incubated at 37 °C for 90 min. After incubation, the wells were washed three times with 150 µL of 1× Wash Buffer. Diluted Capture Antibody solution (50 µL) was added to each well, and the plate was incubated at room temperature for 60 min on an orbital shaker (50–100 rpm).

Then, the wells were aspirated and washed three times with 150 μL of the $1\times$ Wash Buffer. The detection antibody (50 μL) was added to each strip well and incubated at room temperature for 30 min. Then, the wells were washed with 150 μL of the $1\times$ Wash Buffer four times. The enhancer solution (50 μL) was added to each strip well and they were incubated at room temperature for 30 min. Again, the wells were washed with 150 μL of the $1\times$ Wash Buffer four times. The developing solution (100 μL) was added to each well and they were incubated at room temperature for 2–10 min in the dark. The colour change was monitored in the wells where a blue colour developed in the wells with DNMT3B enzyme activity. The stop solution (50 μL) was added to stop the reaction and then absorbance was read on a microplate reader at 450 nm within 5–15 min.

2.8. Statistical Analysis

The data were analysed using statistical software SPSS (IBM SPSS Statistics 21, Hampshire, UK). A one-way analysis of variance (ANOVA) was performed to assess the comparison among the three groups. The threshold for statistical significance was accepted as $p < 0.05$. GraphPad Prism 5 (GraphPad Software, La Jolla, San Diego, CA, USA) was used to graphically display the data. Experimental data are represented as mean \pm standard deviation (SD) and describe a minimum of 3 independent replicates.

3. Results

3.1. Reduced Oxygen Increases Proliferation and Metabolic Activity in hPSC

We determined the proliferation of hPSCs cultured in air oxygen (21% AO) and reduced oxygen conditions (2% PG and 2% WKS) over a 6-day period. A significant increase in proliferation between days 2 and 6 in physoxia settings was noted in comparison to those cultured in air oxygen (AO, $p < 0.05$). Their metabolic activity was explored via MTT and Alamar blue assays. A significant increase was again noted for hPSCs cultured in physoxia when compared to AO ($p < 0.05$). SHEF1 and ZK2012L displayed a significant increase in MTT after day 3 while SHEF2 cells displayed a significant increase in MTT after day 5. Alamar blue indicated increased metabolic activity and the proliferation of cells cultured under both reduced oxygen conditions from day 4 (Figure S1).

3.2. Increased Expression of TRA-160 in Physoxia Cultured hPSCs

The expression of SSEA-4, TRA-1-60 (pluripotency markers) and SSEA-1 (differentiation marker) was then explored via flow cytometry in undifferentiated hPSCs (day 0). As we expected, hPSCs displayed low levels of SSEA-1 expression coupled with high levels of SSEA-4 and TRA-1-60. No significant difference between the conditions for SSEA-4 and SSEA-1 were observed. However, we noted significantly higher expression of TRA-1-60 in SHEF1 cells cultured in 2% PG ($88.41\% \pm 1.79$, $p > 0.01$), SHEF2 cells in 2% WKS ($85.64\% \pm 1.26$, $p > 0.01$) and ZK2012L cells in 2% PG, 2% WKS ($76.84\% \pm 10.84$, $p > 0.01$ and $69.61\% \pm 9.77$, $p > 0.05$) versus 21% AO ($67.23\% \pm 10.57$, $62.71\% \pm 18.18$ and $53.48\% \pm 7.66$) (Figure 1).

3.3. Elevated OCT-4 and SOX-2 Expression in Physoxia Cultured hPSCs

The expression of pluripotency factors OCT-4, NANOG and SOX2 was assessed transcriptionally in different oxygen conditions (21% AO, 2% PG and 2% WKS). OCT-4 expression was increased in 2% PG and 2% WKS in undifferentiated SHEF1 (1.30 ± 0.23 and 1.76 ± 0.50 , respectively), SHEF2 (1.10 ± 0.23 and 1.51 ± 0.10 , respectively), and ZK2012L (1.84 ± 0.20 and 1.64 ± 0.21 , $p > 0.01$, respectively) compared with AO. During differentiation, OCT-4 expression decreased in differentiated SHEF1 and SHEF2 at days 5, 10, and 20 in physoxia. SHEF1 and SHEF2 differentiated in 2% PG showed significant decreases at day 20 (0.33 ± 0.28 and 0.30 ± 0.16 , $p > 0.01$, respectively) and SHEF2 in 2% WKS at day 5 and 20 (0.66 ± 0.11 , $p > 0.05$ and 0.38 ± 0.19 , $p > 0.01$) displayed a significant reduction compared to 21% AO. Undifferentiated ZK2012L cells showed increased OCT-4 expression in 2% PG and 2% WKS (1.83 ± 0.20 and 1.64 ± 0.21 , $p > 0.01$). The pooled hPSCs data

indicated a significant increase in OCT-4 expression in undifferentiated cells in 2% WKS (1.64 ± 0.13 , $p > 0.05$) in comparison to AO with a decreased expression at differentiation days 5, 10, and 20. NANOG expression decreased in PSCs cultured in reduced oxygen environments in undifferentiated and 5-days differentiated SHEF1, SHEF2, and ZK2012L versus AO, and significantly in undifferentiated SHEF1 in 2% PG (0.51 ± 0.31 , $p > 0.05$). The pooled data indicated that NANOG expression was significantly lower in undifferentiated cells cultured in 2% PG and 2% WKS (0.57 ± 0.1 and 0.64 ± 0.11 , $p > 0.01$, respectively) and after 5 days differentiation in 2% PG (0.63 ± 0.09 , $p > 0.05$) compared to AO. An overall increase in SOX-2 expression was noted in PSCs cultured in reduced oxygen conditions. There was a significant increase in undifferentiated SHEF1 and SHEF2 cells cultured in 2% WKS (2.08 ± 0.62 and 1.55 ± 0.19 , $p > 0.05$). Additionally, 10-days differentiated ZK2012L displayed a significant elevation in 2% WKS (2.98 ± 1.01 , $p > 0.05$) versus AO. The pooled hPSC data indicated significantly elevated SOX-2 expression in undifferentiated cells cultured in a 2% WKS environment (1.96 ± 0.36 , $p > 0.01$) in comparison to AO (Figure 2).

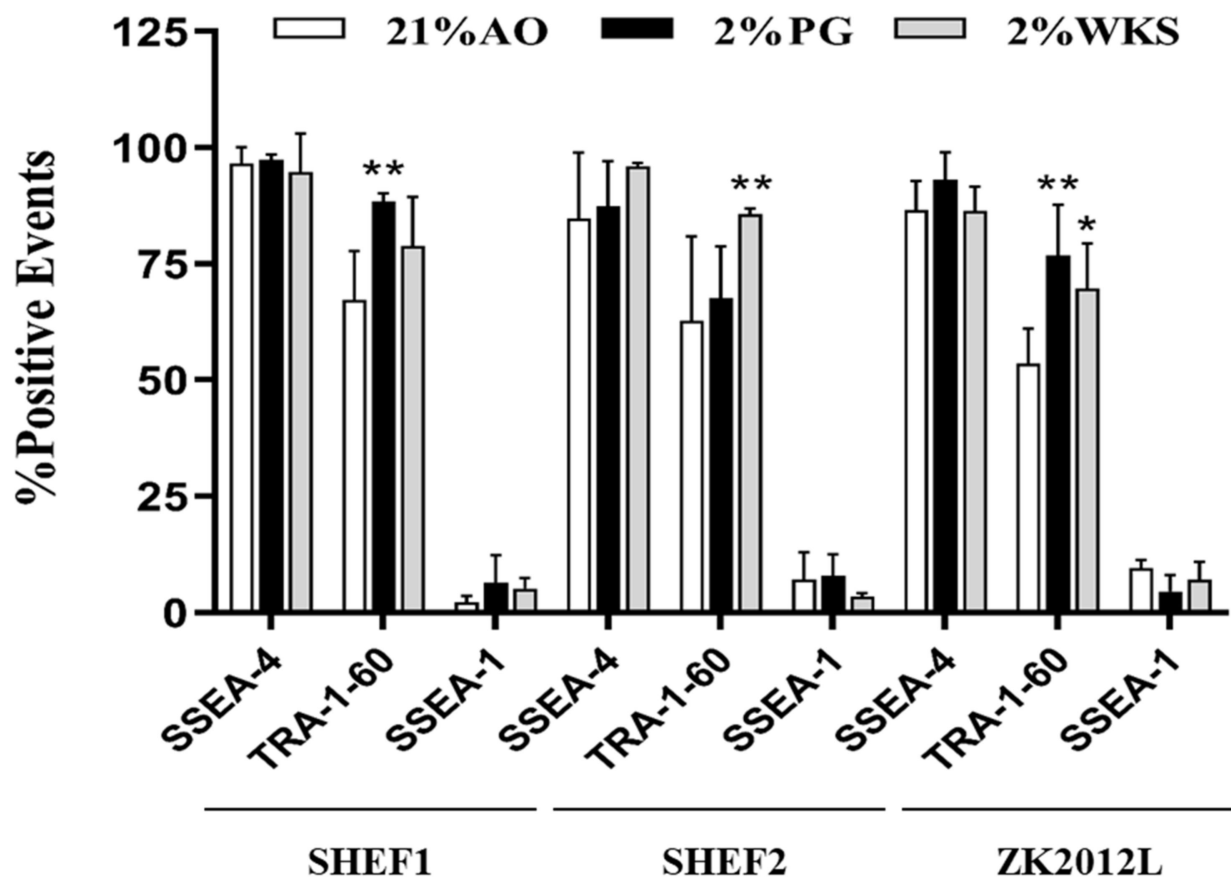


Figure 1. Immunophenotypic characterisation of PSCs. Flow cytometry-based evaluation of expression of pluripotency markers. All PSCs were analysed for SSEA-4, TRA-1-60, SSEA-1 expression in both reduced oxygen (2% PG and 2% WKS) and 21% AO conditions. Y-axis indicates sample names and surface markers. The X-axis shows percentage of positive events. Data are presented as a mean ($n = 3$), * $p < 0.05$, ** $p < 0.01$ vs. 21% AO, and error bar indicates standard deviation (SD).

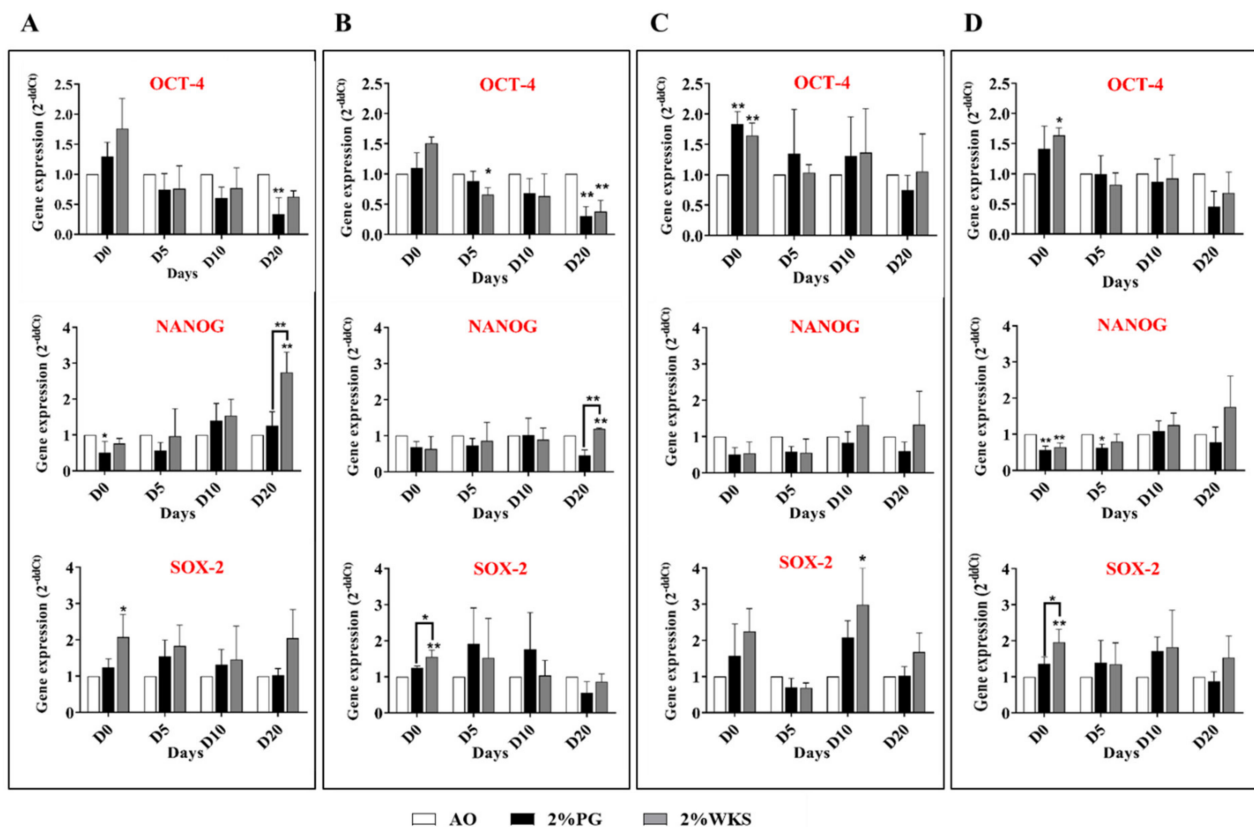


Figure 2. QRT-PCR analysis of OCT-4, SOX-2 and NANOG expression. (A) SHEF1, (B) SHEF2, (C) ZK2012L, and (D) Pooled PSCs-profile, (SHEF1, SHEF2 and ZK2012L). The internal control, ACTB, was used to normalize expression. Y-axis shows the relative changes in $2^{-\Delta\Delta C_T}$ of air oxygen (AO) to physoxia cultured cells. The X-axis indicates time (days). Data are presented as a mean ($n = 3$), * $p < 0.05$, ** $p < 0.01$ vs. 21% AO, connecting lines indicate significance between conditions, and error bars indicate SD.

3.4. Physoxia Decreases Global DNA Methylation in hPSCs

DNA from undifferentiated and differentiated hPSCs was isolated to explore the global DNA methylation levels in 21% AO, 2% PG, and 2% WKS. Decreased global DNA methylation in hPSCs cultured in physoxia (2% PG and 2% WKS) versus 21% AO was noted. Further, global DNA methylation was reduced in a time-dependent manner as differentiation progressed in PSCs.

Undifferentiated SHEF1 cultured in either 2% PG (0.82 ± 0.06 , $p < 0.05$) or 2% WKS (0.73 ± 0.07 , $p < 0.01$) showed significantly decreased 5mC levels versus 21% AO (1.01 ± 0.041). The level of 5mC in day-20 differentiated SHEF1 was significantly decreased in 2% WKS (0.52 ± 0.09 , $p < 0.05$) in comparison to 21% AO (0.72 ± 0.074) (Figure 3A). Undifferentiated and day-20 differentiated SHEF2 in 2% PG displayed significantly decreased 5mC (0.74 ± 0.03 and 0.51 ± 0.02 , $p < 0.05$) versus 21% AO (0.84 ± 0.05 and 0.70 ± 0.08), respectively. There was a significant decrease in the 5mC content at days 10 and 20 in differentiated SHEF2 (0.50 ± 0.03 and 0.41 ± 0.06 , $p < 0.01$) in 2% WKS (Figure 3B).

Undifferentiated ZK2012L cultured in 2% PG (0.98 ± 0.06 , $p < 0.05$) and 2% WKS (0.95 ± 0.05 , $p < 0.05$) showed significantly decreased 5mC levels versus 21% AO (1.22 ± 0.09). Days 5 (0.54 ± 0.05 and 0.54 ± 0.03 , $p < 0.05$) and 20 (0.45 ± 0.05 and 0.43 ± 0.04 , $p < 0.05$) differentiated cells showed a significant reduction in their global 5mC level in 2% PG and 2% WKS, respectively (Figure 3C). The pooled data from three PSCs (SHEF1, SHEF2 and ZK2012L) indicated reduced global 5mC levels in undifferentiated 2% PG and 2% WKS with a significant decrease in 2% WKS at day 20 (0.46 ± 0.5) in comparison to 21% AO (0.69 ± 0.5) (Figure 3D).

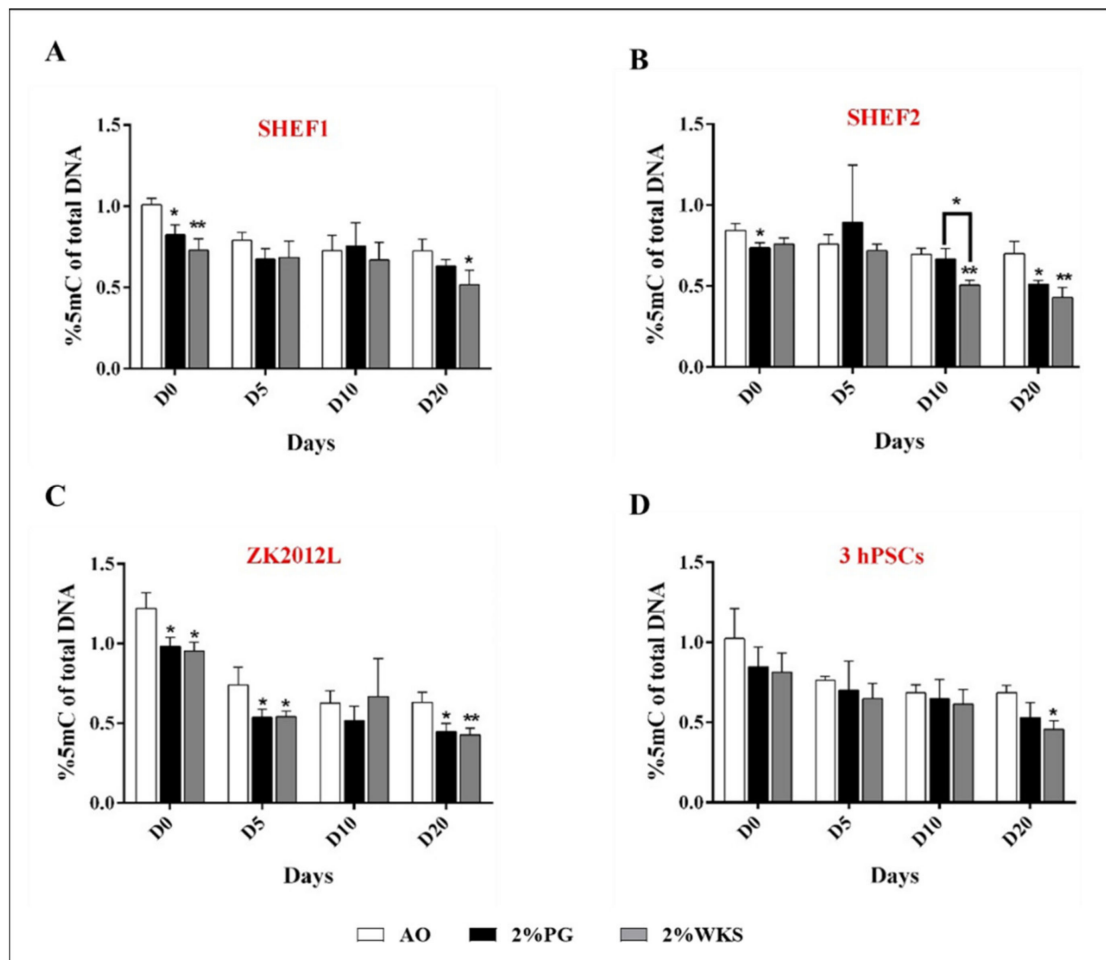


Figure 3. Global 5mC levels in PSCs. (A) SHEF1, (B) SHEF2, (C) ZK2012L, and (D) Pooled PSCs-profile, (SHEF1, SHEF2 and ZK2012L). The methylated DNA fragments of PSCs were analysed using MethylFlash Global DNA Methylation (5-mC) Quantification Kit. Y-axis shows the absorbance (450 nm) of 5-methylcytosine. The X-axis indicates different time points (days). Data are presented as a mean ($n = 3$), * $p < 0.05$, ** $p < 0.01$ vs. 21% AO, connecting lines indicate significance between conditions, and error bars indicate SD.

Significant decreases were observed in the global 5hmC DNA levels of undifferentiated SHEF1 cultured in 2% PG and 2% WKS physoxia environments (0.08 ± 0.006 , $p < 0.05$ and 0.06 ± 0.008 , $p < 0.01$, respectively) compared to AO (0.13 ± 0.03). Significant decreases were observed at days 10 and 20 for differentiation in 2% WKS (0.05 ± 0.01 , $p < 0.05$ and 0.04 ± 0.008 , $p < 0.05$), respectively, versus 21% AO (0.07 ± 0.009) (Figure 4A). Undifferentiated SHEF2 in 2% WKS cells showed a significant decrease (0.14 ± 0.02 , $p < 0.05$) in comparison to cells cultured in 21% AO (0.21 ± 0.03). ZK2012L cultured in 2% WKS showed a significant reduction in the percentage of 5hmC at days 0, 5, and 20 (0.13 ± 0.02 , 0.08 ± 0.02 and 0.06 ± 0.01 , $p < 0.05$, respectively) versus 21% AO (0.21 ± 0.04 , 0.12 ± 0.02 and 0.09 ± 0.02) (Figure 4B). ZK2012L displayed a significant decrease in 2% PG at day 20 (0.06 ± 0.01) in comparison to 21% AO (0.15 ± 0.02) (Figure 4C). Lastly, no significant difference was observed in the pooled PSCs data, but an overall reduction in global 5hmC levels in cells cultured under physoxia was noted in undifferentiated and differentiated cells (Figure 4D).

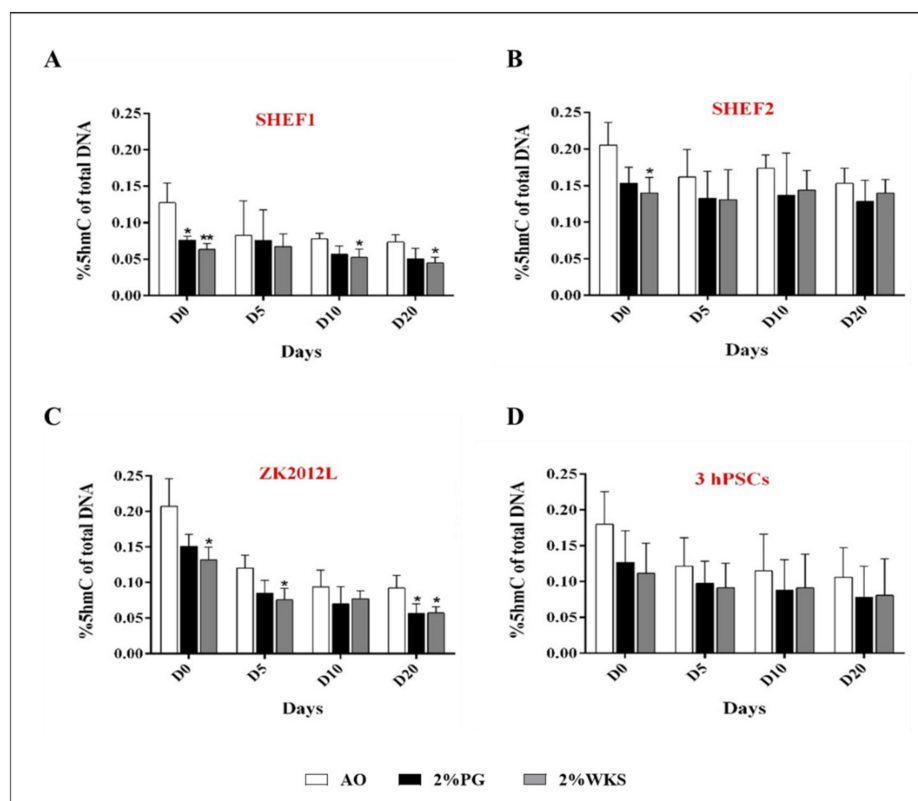


Figure 4. Global 5hmC levels PSCs. (A) SHEF1, (B) SHEF2, (C) ZK2012L, and (D) Pooled PSCs-profile, (SHEF1, SHEF2 and ZK2012L). The methylated DNA fragments of PSCs were analysed using MethylFlash Global Hydroxymethylated DNA (5-hmC) Quantification Kit. Y-axis shows absorbance (450 nm) of 5-hydroxymethylcytosine. The X-axis indicates different time points (days). Data are presented as a mean ($n = 3$), * $p < 0.05$, ** $p < 0.01$ vs. 21% AO, connecting lines indicate significance between conditions, and error bars indicate SD.

3.5. Decreased DNMT3B, TET1 and TET3 Gene Expression Associates with Physoxic Culture

No changes in the expression of DNMT1 or TET2 were noted during the differentiation of hPSCs. DNMT3A expression significantly decreased in differentiated SHEF1 at day 5 in 2% WKS (0.65-fold \pm 0.22, $p < 0.05$) vs. 21% AO. Undifferentiated SHEF2 and ZK2012L cells displayed reduced DNMT3A gene expression in 2% PG and 2% WKS (0.59-fold \pm 0.03 and 0.65-fold \pm 0.13, $p < 0.05$, respectively) in comparison to 21% AO.

Decreased DNMT3B expression was noted in undifferentiated SHEF1 in 2% PG and 2% WKS (0.63-fold \pm 0.21 and 0.48-fold \pm 0.15, $p < 0.05$, respectively), and during spontaneous differentiation at days 5, 10, and 20 in 2% WKS (0.45-fold \pm 0.16, $p < 0.01$, 0.50-fold \pm 0.19 and 0.49-fold \pm 0.21, $p < 0.05$, respectively) versus AO (Figure 5A). Undifferentiated SHEF2 in 2% PG and 2% WKS had reduced DNMT3B expression (0.26-fold \pm 0.18 and 0.38-fold \pm 0.22, $p < 0.01$, respectively), and after 10 days, differentiated (0.52-fold \pm 0.19 and 0.36-fold \pm 0.24, $p < 0.05$, respectively) in 2% PG and 2% WKS and at day 20 in 2% WKS (0.16-fold \pm 0.03, $p < 0.01$) in comparison to those cultured in 21% AO (Figure 5B). Similar reductions were observed in undifferentiated ZK2012L in 2% PG and 2% WKS (0.50-fold \pm 0.14 and 0.45-fold \pm 0.17, $p < 0.01$, respectively), and after 5 (0.66-fold \pm 0.16, $p < 0.05$ and 0.41-fold \pm 0.17, $p < 0.01$, respectively) and 20 days (0.55-fold \pm 0.17) differentiation versus 21% AO (Figure 5C). The pooled data from all the PSCs tested showed a significant reduction in DNMT3B expression in undifferentiated hPSCs cultured in either 2% PG or 2% WKS conditions (0.46 \pm 0.18 and 0.44 \pm 0.05, $p < 0.01$, respectively), and after 20-days differentiation (0.67 \pm 0.07, $p < 0.05$ and 0.40 \pm 0.21, $p < 0.01$, respectively) in comparison to 21% AO (Figure 5D).

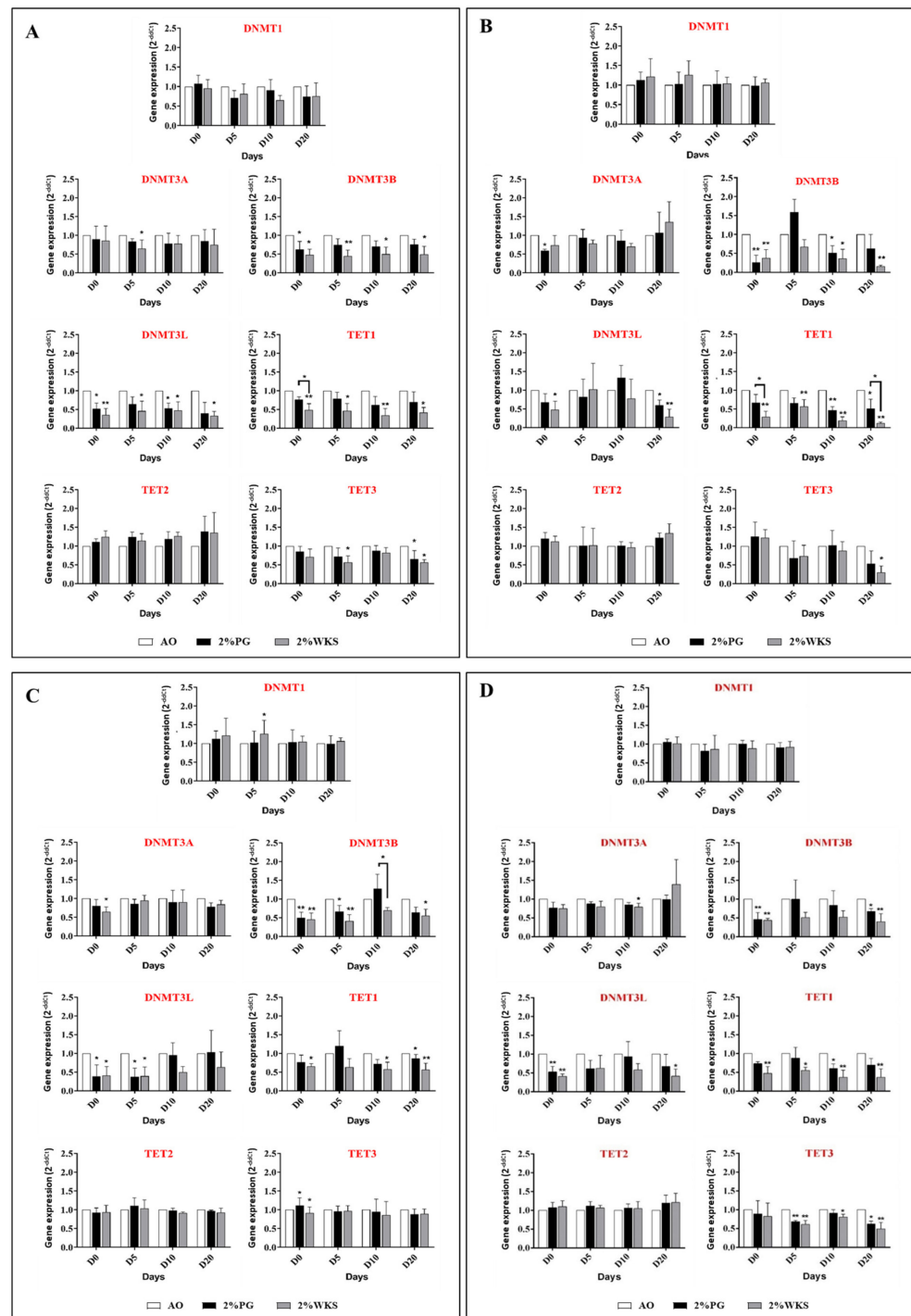


Figure 5. QRT-PCR analysis of DNMTs and TETs in PSCs. Gene expression of DNMTs and TETs was performed (A) SHEF1, (B) SHEF2, (C) ZK2012L, and (D) Pooled PSCs lines, (SHEF1, SHEF2 and ZK2012L) in 21% AO and physiological oxygen conditions (2% PG and 2% WKS). The internal control ACTB was used for normalization. Y-axis shows the relative changes in $2^{-\Delta\Delta CT}$ of air oxygen to physoxia. The X-axis indicates time (days). Data are presented as a mean ($n = 3$), * $p < 0.05$, ** $p < 0.01$ vs. 21% AO, connecting lines indicate significance between conditions, error bars indicate SD.

DNMT3L expression significantly decreased in undifferentiated and 10-days differentiated SHEF1 in 2% PG ($p < 0.05$) and 2% WKS ($p < 0.01$ and $p < 0.05$, respectively), and in 2%WKS at days 5 and 20 ($p < 0.05$) in comparison to 21% AO (Figure 5A). A decreased expression of DNMT3L was noted in undifferentiated 2% WKS ($p < 0.05$) and 20-days differ-

entiated SHEF2 in 2% PG ($p < 0.05$) and 2% WKS ($p < 0.01$) (Figure 5B). Further, DNMT3L expression was decreased in undifferentiated ($p < 0.05$), and day-5 differentiated ZK2012L cells ($p < 0.05$) in both 2% PG and 2% WKS (Figure 5C). The pooled data from all three PSCs showed a significant reduction ($p < 0.01$) in DNMT3L expression in undifferentiated hPSCs cultured in both 2% PG and 2% WKS and day 20 differentiated cells in 2% WKS ($p < 0.05$) (Figure 5D).

TET1 expression was reduced in undifferentiated SHEF1 (0.49-fold \pm 0.17, $p < 0.01$), and 5- (0.46-fold \pm 0.19, $p < 0.05$), 10 (0.34-fold \pm 0.18, $p < 0.01$) and 20-days differentiation (0.41-fold \pm 0.14, $p < 0.05$) in 2% WKS in comparison to AO (Figure 5A). TET1 expression was reduced in undifferentiated SHEF2 in 2% WKS (0.29-fold \pm 0.15, $p < 0.01$), day 5 (0.57-fold \pm 0.18, $p < 0.01$), day 10 (0.20-fold \pm 0.10, $p < 0.01$), and day 20 (0.13-fold \pm 0.03, $p < 0.01$) differentiation, and in 2% PG at day 10 (0.47-fold \pm 0.09, $p < 0.01$) and day 20 (0.51-fold \pm 0.24, $p < 0.05$) (Figure 5B). TET1 expression in ZK2012L cells was decreased in undifferentiated cells (0.65-fold \pm 0.08, $p < 0.05$) and day-10 differentiated cells (0.57-fold \pm 0.19, $p < 0.05$) in 2% WKS, and in day 20 with both 2% PG and 2% WKS (0.87-fold \pm 0.10, $p < 0.05$ and 0.57-fold \pm 0.17, $p < 0.01$, respectively) (Figure 5C). The pooled PSC data indicated a significant decrease in TET1 expression in undifferentiated ($p < 0.01$) and differentiated cells at days 5 ($p < 0.05$), 10, and 20 ($p < 0.01$) in 2% WKS and following 10-days differentiation in 2% PG ($p < 0.05$) versus AO (Figure 5D).

Finally, TET3 expression was significantly reduced in day-5 differentiated SHEF1 ($p < 0.05$) in 2% WKS and day 20 in 2% PG and 2% WKS ($p < 0.05$) in comparison to those cultured in 21% AO. Significant decreases in day-20-differentiated SHEF2 cultured in 2% WKS ($p < 0.05$) and undifferentiated ZK2012L cells with 2% PG and 2% WKS ($p < 0.05$) were also noted in comparison to AO. The pooled hPSCs data demonstrated decreased TET3 expression at day-5 ($p < 0.01$), day 10 ($p < 0.05$), and day-20 ($p < 0.01$) differentiation in 2% WKS, and both days 5 ($p < 0.01$) and 20 in 2% PG (Figure 5).

3.6. DNMT3B Enzyme Activity after Differentiation of PSCs

We used the EpiQuik™ DNMT3B Activity Assay Kit to screen DNMT3B enzyme activity during differentiation. There was a slight decrease at day 5. Differentiated cells in 2% WKS demonstrated decreased enzyme activity at day 10 (0.64 \pm 0.06, $p < 0.05$), day 20 (0.54 \pm 0.05, $p < 0.01$) and day 40 (0.48 \pm 0.09, $p < 0.001$) (Figure 6). The DNMT3B results were consistent with reduced global methylation in differentiated cells in a time-dependent manner.

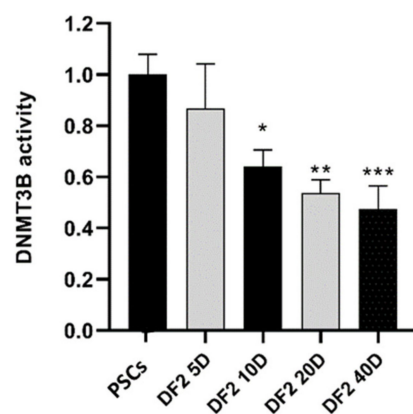


Figure 6. DNMT3B enzyme activity in PSCs in 2% WKS. Protein samples were isolated from undifferentiated and 5, 10, 20, 40 days differentiated cells exposed to physoxia conditions. The absorbance values of differentiated cells were normalised to undifferentiated sample. Data are presented as a mean ($n = 3$), * $p < 0.05$, ** $p < 0.01$, *** $p < 0.001$.

3.7. Physoxia Increased DNMT3B and DNMT3L Promoter Methylation in hPSCs

The mean level of DNMT3B promoter methylation was higher in undifferentiated SHEF1 in 2% PG (23%, $p < 0.05$) and 2% WKS (32%, $p < 0.01$) versus 21% AO (11%). The

methylation levels of the DNMT3B promoter were also elevated at differentiation days 5 in 2% PG and 20 in 2% WKS (25%, $p < 0.05$ and 25%, $p < 0.01$) compared to 21% AO (13% and 11%). The percentage of DNMT3L promoter methylation was significantly higher in undifferentiated (86%, $p < 0.01$) and day-10 (90%, $p < 0.05$) and 20 (90%, $p < 0.01$) differentiated cells in 2% WKS compared with 21% AO (70%, 75% and 73%, respectively) (Figure 7A).

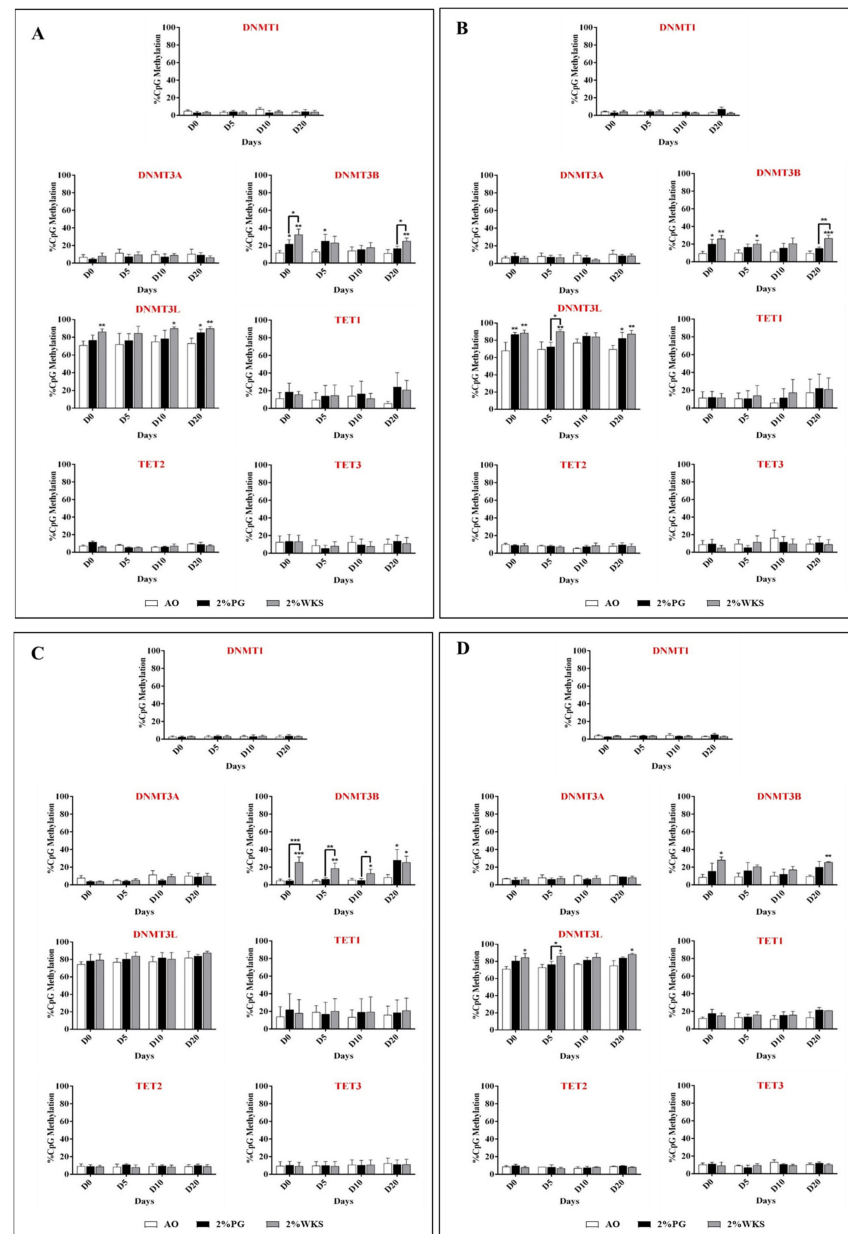


Figure 7. DNMT and TET promoter methylation in PSCs. (A) SHEF1 and (B) SHEF2, (C) ZK2012L, and (D) Pooled PSCs (SHEF1, SHEF2 and ZK2012L). CpG island methylation in DNMTs and TETs promoters were evaluated using pyrosequencing. Y-axis represents DNA methylation percentage at CpG regions. The X-axis represents time (days). Data are presented as mean ($n = 3$), * $p < 0.05$, ** $p < 0.01$ and *** $p < 0.001$ vs. 21% AO, connecting lines indicate significance between conditions, and error bars indicate SD.

A significant increase in DNMT3B promoter methylation was noted in undifferentiated SHEF2 cells cultured in 2% PG (20%, $p < 0.05$) and 2% WKS (26%, $p < 0.01$) versus 21% AO (9%). In addition, there was a significant elevation in methylation at days 5 (20%, $p < 0.05$)

and 20 (27%, $p < 0.01$) in 2% WKS compared with 21% AO (10% and 9%, respectively). Furthermore, DNMT3L showed a significant increase in methylation in 2% PG (87%, $p < 0.01$) and 2% WKS (89%, $p < 0.01$) in undifferentiated SHEF2 cells compared with 21% AO (68%). There was a significant increase in methylation levels at day 5 (90%, $p < 0.01$) and 20 in 2%PG and 2%WKS (82%, $p < 0.05$ and 87%, $p < 0.01$, respectively) compared with 21% AO (70%) (Figure 7B).

Undifferentiated ZK2012L (26%, $p < 0.001$) and differentiated cells at day 5 (19%, $p < 0.01$), 10 (13%, $p < 0.05$), and 20 (25%, $p < 0.05$) cultured in 2% WKS had significantly higher DNMT3B-promoter methylation levels compared with 21% AO (5%, 4%, 5% and 8%, respectively). No significant change was noted in the methylation of DNMT3L for ZK2012L cells (Figure 7C). The combined data from three PSCs revealed that there was a significant increase in undifferentiated (28%, $p < 0.05$) and day-20 differentiated (26%, $p < 0.01$) cells cultured under 2% WKS versus 21% AO (10% and 8%). A significant increase was noted in DNMT3L methylation in undifferentiated cells and in day-5 and 20 differentiation (85%, 86% and 88%, $p < 0.05$) in the 2% WKS conditions in comparison to 21% AO (71%, 73% and 75%), respectively. In general, no significant change was noted in the promoter methylation level of DNMT1, DNMT3A, TET1, TET2 and TET3 genes in either SHEF1, SHEF2, or ZK2012L cells (Figure 7D).

3.8. Physoxia Increased HIF2A Gene Expression in PSCs

Undifferentiated SHEF1 displayed a significant downregulation of HIF1A transcript in physoxia (2%PG and 2%WKS, $p < 0.01$), and at days 5 ($p < 0.01$ and $p < 0.05$, respectively), 10 ($p < 0.05$), and 20 of differentiation ($p < 0.01$ and $p < 0.05$, respectively), vs. 21% AO (Figure 8A). A significant decrease was noted in the gene expression of HIF1A in undifferentiated SHEF2, and on days 5, 10 and 20 after differentiation ($p < 0.05$) in 2% PG, and 5, 10 and 20 days after the differentiation of SHEF2 in 2% WKS ($p < 0.01$, $p < 0.01$ and $p < 0.05$, respectively) (Figure 8B). We also noted a significant decrease in undifferentiated ZK2012L ($p < 0.01$, $p < 0.01$), and at differentiation days 5 ($p < 0.05$, $p < 0.01$), 10 ($p < 0.05$, $p < 0.01$) and 20 ($p < 0.01$, $p < 0.01$) in 2% PG and 2% WKS in comparison to 21% AO (Figure 8C). No significant changes to HIF2A gene expression in SHEF1 or SHEF2 were noted. ZK2012L displayed an increased expression of HIF2A in undifferentiated and day-5 differentiated cells ($p < 0.05$) in 2% PG only (Figure 8).

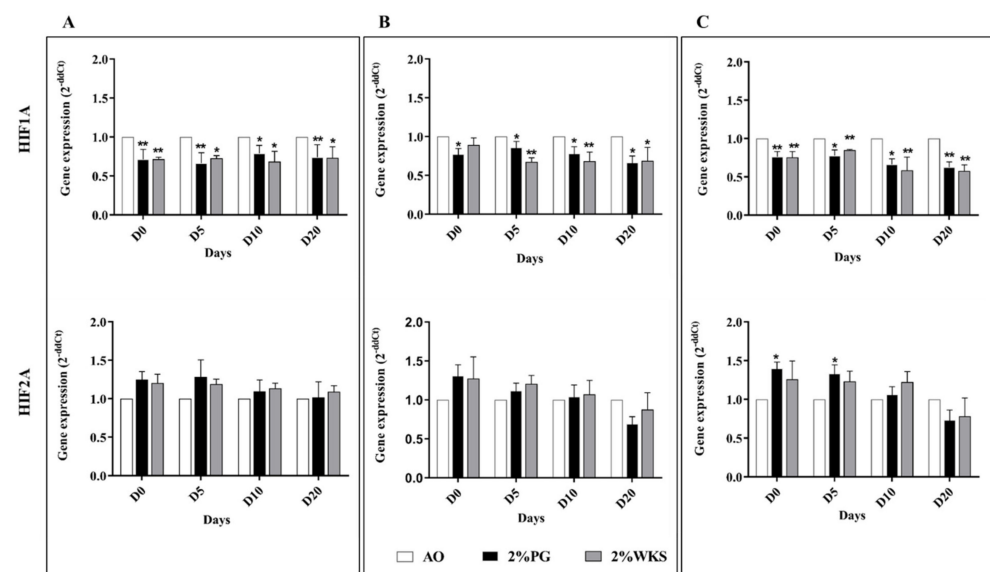


Figure 8. Gene expression of HIF1A and HIF2A in (A) SHEF1, (B) SHEF2, and (C) ZK2012L. The RT-qPCR expression of the HIFs normalized to the expression of internal control ACTB. Y-axis shows the relative changes in $2^{-\Delta\Delta CT}$ of air oxygen exposed cells to physoxia cultured cells. The X-axis indicates time (days). Data are presented as a mean ($n = 3$), * $p < 0.05$, ** $p < 0.01$.

4. Discussion

Epigenetics marks including DNA methylation (5mC and 5hmC) impact cellular characteristics and fate, and are critical for various cellular processes [36]. The role of the methylation of Cytosine residues (5mC) at CpG islands is well studied across a range of biological processes including gene expression, cell differentiation, and development [37]; however, 5hmC is still being explored in cell differentiation and transcriptional regulation in mammalian cells [38]. Oxygen variations can mediate stem cell fate, where, for example, low, physiologic, oxygen conditions increase clonal recovery, maintain a higher number of colony-initiating cells, alter metabolism and morphology, and enhance the proliferation and stemness of PSCs [22,23,25,39]. Here, we focused on the role of physoxia on PSC characteristics in conjunction with global DNA methylation, the regulation of methylation enzymes, and the methylation of their promoters in human PSCs. We determined, in agreement with others, that reduced oxygen conditions enhanced the proliferation and metabolic activity of PSCs when compared to air-oxygen cultured cells [19,40]. We observed that global methylation is oxygen-sensitive and associated with the regulation of DNMT3B transcription and translation.

Immunocytochemistry and flow cytometry demonstrated that undifferentiated PSCs expressed the anticipated pluripotency markers, namely OCT-4, NANOG, ALP, SSEA-4, TRA-1-60, and were negative for SSEA-1. Previous reports suggested that reduced-oxygen culture conditions have no detrimental effect on the expression of stem cell markers in PSCs [19,23,41,42]. We noted elevated OCT-4 and SOX-2, although not NANOG, expression in 2% WKS condition with flow cytometry determining increased TRA-1-60 expression in reduced oxygen conditions. Therefore, we believe that a controlled oxygen environment of 2% WKS provides a more consistent environment for PSCs than 2% PG. Consistent with our observations, hESCs exposed to AO displayed the decreased proliferation and reduced expression of the SOX2, NANOG, and OCT4 gene and protein expression when compared with those cultured at 5% O₂ tri-gas incubators [19,43]. In contrast to the above, other reports detail no significant differences in SOX2, NANOG, or OCT4 expression in hESCs cultured at 2–4% O₂ (again with tri-gas incubators) compared to AO [44,45].

DNA methylation and hydroxymethylation have essential roles in PSC functioning and in the characteristic determination of physiological oxygen conditions [29,46]. Oxygen can alter the global epigenetic landscape, for instance, global histone methylation was decreased at 5% oxygen tension in hPSCs [47]. These observations are consistent with ours, in which we noted decreased global methylation (vs. AO) in 5mC and 5hmC levels in undifferentiated hPSCs exposed to physiological oxygen conditions (2% PG and 2% WKS). Recent reports detail that both 5mC and 5hmC levels are high in ESCs and that these reduce after differentiation [17,48–51]. Furthermore, essential transcription factors involved in the ESCs maintenance of pluripotency such as OCT-4 and NANOG are unmethylated in undifferentiated cells and become methylated as differentiation progresses [27,52,53]. We also noted progressively decreased global 5mC and 5hmC levels during the differentiation of PSCs and reduced global methylation in physiological oxygen conditions (2% PG and 2% WKS) in differentiated stem cells compared to AO.

Notably, global methylation levels correlated with decreased DNMT3B and TET1 expression in reduced oxygen conditions. ESCs exhibit robust de novo methyltransferase enzyme (DNMT3A and DNMT3B) expression when undifferentiated, with levels of DNMT3B decreasing with progressive differentiation states [16,54–56]. A previous report described that the expression of DNMT3B decreased at 5% oxygen in undifferentiated hPSCs [47]. Consistent with this, we noted reduced DNMT3B expression in physiological oxygen conditions in undifferentiated hPSCs and subsequently differentiated cells. Methylation levels in the DNMT3B promoter were significantly higher under reduced oxygen settings when compared to AO. CpG island methylation can impair transcription factor binding, recruit repressive methyl-binding proteins, and stably silence gene expression [26]. Global methylation levels and DNMT3B enzyme activity decreased by almost two times after 20 days differentiation in three oxygen conditions with a gradual decrease in both global

methylation and DNMT3B enzyme activity observed across this time course. Decreased global methylation levels in physoxic culture were accompanied by reduced DNMT3B, TET1 and TET3 gene expression. Taken together, we evidenced the reduced transcriptional expression of DNMT3B in association with increased methylation of its promoter. In contrast, there was a significant decrease in the TET1 mRNA level but no significant changes occurred for its promoter CpG content in physoxia versus AO.

Long term exposure of hESC to low oxygen decreased the expression of HIF1A mRNA in hESCs [19]. We also noted decreased HIF1A gene expression in physoxia. In contrast, the long-term physoxic culture resulted in upregulated HIF2A at transcript levels. Consistent with this observation, previous reports detailed that HIF2A was upregulated following the long-term culture of hESC in 5% O₂ when compared with air-cultured counterparts [19]. Further, and indicative of a conserved behaviour, HIF2A was upregulated at transcriptional and translational levels in human MSCs in a 5% O₂ culture setting [57]. The repression of HIF2A via siRNA resulted in the decreased proliferation and reduced expression of OCT-4, NANOG and SOX-2 in hESCs cultured under 5% O₂ [19]. In addition, DNMT1 and DNMT3B promoters each displayed hypoxia response elements to HIF binding [33,46]. Therefore, we hypothesise that increased HIF2A and reduced HIF1A under physoxia may associate with, or even drive, the observed decrease in DNMT3B and overall increase its promoter methylation.

In summary, we demonstrated that the physiological oxygen tension increased pluripotency marker expression, proliferation, and metabolic activity with a concurrent decrease in DNMT3B, TET1 gene expression, and global DNA methylation in hPSCs. Further, DNMT3B expression was methylation-regulated in an oxygen-sensitive manner. We show that physoxia conditions modify levels of global methylation linked to DNMT3B expression and that hPSCs display oxygen-sensitive methylation patterns. Importantly, air oxygen is almost never normoxic in mammalian cell culture and increased global methylation can be considered as an artefact of air oxygen culture. Physoxia is an essential component for regenerative medicine to safely realise cell potential and facilitate clean characterisation. Our previous data showed no impact of low oxygen conditions at the histology level in PSCs, but we observed transcriptional changes, which led us to explore molecular alterations in greater detail. Here, we used spontaneous differentiation as a model but there are limitations to this approach as an experimental tool. Future studies may, for example, explore differentiation markers and methylation changes in induced or directed differentiated cells in different oxygen settings. In addition, *in vivo* differentiation models can be utilised to explore other essential epigenetic markers including histone modifications that may contribute to an enhanced understanding of epigenetics in embryonic development in physoxia.

Supplementary Materials: The following supporting information can be downloaded at: <https://www.mdpi.com/article/10.3390/ijms23105854/s1>.

Author Contributions: Conceptualization, R.M.K.A., F.D. and N.R.F.; Data curation, F.D.; Formal analysis, F.D. and R.M.K.A.; Funding acquisition, R.M.K.A. and N.R.F.; Investigation, N.R.F.; Methodology, R.M.K.A., F.D., N.R.F. and M.K.; Project administration, R.M.K.A. and N.R.F.; Supervision, N.R.F.; Validation, M.K. and N.R.F.; Visualization, F.D.; Writing—original draft, F.D.; Writing—review & editing, F.D. All authors have read and agreed to the published version of the manuscript.

Funding: This research was funded by the Iraqi Ministry of Higher Education and Scientific Research, University of Baghdad, Baghdad, Iraq, RMKAJ (S1453) and 2) Turkish Ministry of National Education to FD.

Institutional Review Board Statement: Not applicable.

Informed Consent Statement: Not applicable.

Data Availability Statement: Data available in a publicly accessible repository.

Acknowledgments: The work described in this paper was principally funded by the Iraqi Ministry of Higher Education and Scientific Research, University of Baghdad, RMKAJ (S1453), Baghdad, Iraq. We also wish to thank the Turkish Ministry of National Education for their support.

Conflicts of Interest: The authors declare no conflict of interest.

Abbreviations

5-Methylcytosine (5mC) and 5-hydroxymethylcytosine (5hmC); pluripotent stem cells (PSCs); embryonic stem cells (ESCs); mesenchymal stem cells (MSCs); hypoxia-inducible factor (HIF)-1; bone marrow (BM); DNA Methyltransferase (DNMT); Histone deacetylases (HDAC); Ten eleven translocation (TET) enzymes.

References

1. Yagi, M.; Yamanaka, S.; Yamada, Y. Epigenetic foundations of pluripotent stem cells that recapitulate in vivo pluripotency. *Lab. Investig.* **2017**, *97*, 1133–1141. [CrossRef] [PubMed]
2. Loh, Y.-H.; Ng, J.-H.; Ng, H.-H. Molecular framework underlying pluripotency. *Cell Cycle* **2008**, *7*, 885–891. [CrossRef] [PubMed]
3. Boyer, L.A.; Mathur, D.; Jaenisch, R. Molecular control of pluripotency. *Curr. Opin. Genet. Dev.* **2006**, *16*, 455–462. [CrossRef] [PubMed]
4. Abu-Dawud, R.; Graffmann, N.; Ferber, S.; Wruck, W.; Adjaye, J. Pluripotent stem cells: Induction and self-renewal. *Philos. Trans. R. Soc. B Biol. Sci.* **2018**, *373*, 20170213. [CrossRef] [PubMed]
5. Takahashi, K.; Tanabe, K.; Ohnuki, M.; Narita, M.; Ichisaka, T.; Tomoda, K.; Yamanaka, S. Induction of Pluripotent Stem Cells from Adult Human Fibroblasts by Defined Factors. *Cell* **2007**, *131*, 861–872. [CrossRef] [PubMed]
6. Tavakoli, T.; Xu, X.; Derby, E.; Serebryakova, Y.; Reid, Y.; Rao, M.S.; Mattson, M.P.; Ma, W. Self-renewal and differentiation capabilities are variable between human embryonic stem cell lines I3, I6 and BG01V. *BMC Cell Biol.* **2009**, *10*, 44. [CrossRef] [PubMed]
7. Narsinh, K.H.; Plews, J.; Wu, J.C. Comparison of Human Induced Pluripotent and Embryonic Stem Cells: Fraternal or Identical Twins? *Mol. Ther.* **2011**, *19*, 635–638. [CrossRef]
8. Bibikova, M.; Chudin, E.; Wu, B.; Zhou, L.; Garcia, E.W.; Liu, Y.; Shin, S.; Plaia, T.W.; Auerbach, J.M.; Arking, D.E.; et al. Human embryonic stem cells have a unique epigenetic signature. *Genome Res.* **2006**, *16*, 1075–1083. [CrossRef]
9. Fouse, S.D.; Shen, Y.; Pellegrini, M.; Cole, S.; Meissner, A.; Van Neste, L.; Jaenisch, R.; Fan, G. Promoter CpG Methylation Contributes to ES Cell Gene Regulation in Parallel with Oct4/Nanog, PcG Complex, and Histone H3 K4/K27 Trimethylation. *Cell Stem Cell* **2008**, *2*, 160–169. [CrossRef]
10. Guil, S.; Esteller, M. DNA methylomes, histone codes and miRNAs: Tying it all together. *Int. J. Biochem. Cell Biol.* **2009**, *41*, 87–95. [CrossRef]
11. Portela, A.; Esteller, M. Epigenetic modifications and human disease. *Nat. Biotechnol.* **2010**, *28*, 1057–1068. [CrossRef]
12. Cheng, X.; Blumenthal, R.M. Mammalian DNA Methyltransferases: A Structural Perspective. *Structure* **2008**, *16*, 341–350. [CrossRef]
13. Okano, M.; Bell, D.W.; Haber, D.A.; Li, E. DNA Methyltransferases Dnmt3a and Dnmt3b Are Essential for De Novo Methylation and Mammalian Development. *Cell* **1999**, *99*, 247–257. [CrossRef]
14. Song, J.; Rechkoblit, O.; Bestor, T.H.; Patel, D.J. Structure of DNMT1-DNA Complex Reveals a Role for Autoinhibition in Maintenance DNA Methylation. *Science* **2011**, *331*, 1036–1040. [CrossRef]
15. Turek-Plewa, J.; Jagodziński, P.P. The Role of Mammalian DNA Methyltransferases in the Regulation of Gene Expression. 2005, Volume 10. Available online: <http://www.cmbi.org.pl> (accessed on 12 December 2021).
16. Liao, J.; Karnik, R.; Gu, H.; Ziller, M.J.; Clement, K.; Tsankov, A.M.; Akopian, V.; Gifford, C.A.; Donaghey, J.; Galonska, C.; et al. Targeted disruption of DNMT1, DNMT3A and DNMT3B in human embryonic stem cells. *Nat. Genet.* **2015**, *47*, 469–478. [CrossRef]
17. Jackson, M.; Krassowska, A.; Gilbert, N.; Chevassut, T.; Forrester, L.; Ansell, J.; Ramsahoye, B. Severe Global DNA Hypomethylation Blocks Differentiation and Induces Histone Hyperacetylation in Embryonic Stem Cells. *Mol. Cell. Biol.* **2004**, *24*, 8862–8871. [CrossRef]
18. Tadokoro, Y.; Ema, H.; Okano, M.; Li, E.; Nakauchi, H. De novo DNA methyltransferase is essential for self-renewal, but not for differentiation, in hematopoietic stem cells. *J. Exp. Med.* **2007**, *204*, 715–722. [CrossRef]
19. Forristal, C.E.; Wright, K.L.; Hanley, N.A.; Oreffo, R.O.C.; Houghton, F.D. Hypoxia inducible factors regulate pluripotency and proliferation in human embryonic stem cells cultured at reduced oxygen tensions. *Reproduction* **2010**, *139*, 85–97. [CrossRef]
20. Ma, T.; Grayson, W.L.; Fröhlich, M.; Vunjak-Novakovic, G. Hypoxia and stem cell-based engineering of mesenchymal tissues. *Biotechnol. Prog.* **2009**, *25*, 32–42. [CrossRef]

21. Chen, C.; Tang, Q.; Zhang, Y.; Yu, M.; Jing, W.; Tian, W. Physioxia: A more effective approach for culturing human adipose-derived stem cells for cell transplantation. *Stem Cell Res. Ther.* **2018**, *9*, 148. [[CrossRef](#)]
22. Prado-Lopez, S.; Conesa, A.; Armiñán, A.; Martínez-Losa, M.; Escobedo-Lucea, C.; Gandia, C.; Tarazona, S.; Melguizo, D.; Blesa, D.; Montaner, D.; et al. Hypoxia Promotes Efficient Differentiation of Human Embryonic Stem Cells to Functional Endothelium. *Stem Cells* **2010**, *28*, 407–418. [[CrossRef](#)]
23. Forsyth, N.R.; Musio, A.; Vezzoni, P.; Simpson, A.H.R.; Noble, B.S.; McWhir, J. Physiologic Oxygen Enhances Human Embryonic Stem Cell Clonal Recovery and Reduces Chromosomal Abnormalities. *Cloning Stem Cells* **2006**, *8*, 16–23. [[CrossRef](#)] [[PubMed](#)]
24. Dunwoodie, S.L. The Role of Hypoxia in Development of the Mammalian Embryo. *Dev. Cell* **2009**, *17*, 755–773. [[CrossRef](#)] [[PubMed](#)]
25. Csete, M. Oxygen in the cultivation of stem cells. In *Annals of the New York Academy of Sciences*; New York Academy of Sciences: New York, NY, USA, 2005; Volume 1049, pp. 1–8. [[CrossRef](#)]
26. Mohn, F.; Weber, M.; Rebhan, M.; Roloff, T.C.; Richter, J.; Stadler, M.B.; Bibel, M.; Schübeler, D. Lineage-Specific Polycomb Targets and De Novo DNA Methylation Define Restriction and Potential of Neuronal Progenitors. *Mol. Cell* **2008**, *30*, 755–766. [[CrossRef](#)] [[PubMed](#)]
27. Altun, G.; Loring, J.; Laurent, L.C. DNA methylation in embryonic stem cells. *J. Cell. Biochem.* **2010**, *109*, 1–6. [[CrossRef](#)] [[PubMed](#)]
28. Shahrzad, S.; Bertrand, K.; Minhas, K.; Coomber, B.L. Induction of DNA Hypomethylation by Tumor Hypoxia. *Epigenetics* **2007**, *2*, 119–125. [[CrossRef](#)]
29. Mariani, C.J.; Vasanthakumar, A.; Madzo, J.; Yesilkamal, A.; Bhagat, T.; Yu, Y.; Verma, A. TET1-Mediated Hydroxymethylation Facilitates Hypoxic Gene Induction in Neuroblastoma. *Cell Rep.* **2014**, *7*, 1343–1352. [[CrossRef](#)]
30. Dogan, F.; Aljumaily, R.; Kitchen, M.; Forsyth, N. DNMT3B Is an Oxygen-Sensitive De Novo Methylase in Human Mesenchymal Stem Cells. *Cells* **2021**, *10*, 1032. [[CrossRef](#)]
31. Cheng, Y.; Xie, N.; Jin, P.; Wang, T. DNA methylation and hydroxymethylation in stem cells. *Cell Biochem. Funct.* **2015**, *33*, 161–173. [[CrossRef](#)]
32. Burr, S.; Caldwell, A.; Chong, M.; Beretta, M.; Metcalf, S.; Hancock, M.; Arno, M.; Balu, S.; Kropf, V.L.; Mistry, R.K.; et al. Oxygen gradients can determine epigenetic asymmetry and cellular differentiation via differential regulation of Tet activity in embryonic stem cells. *Nucleic Acids Res.* **2018**, *46*, 1210–1226. [[CrossRef](#)]
33. Skowronski, K.; Dubey, S.; Rodenhiser, D.I.; Coomber, B. Ischemia dysregulates DNA methyltransferases and p16INK4 methylation in human colorectal cancer cells. *Epigenetics* **2010**, *5*, 547–556. [[CrossRef](#)]
34. Watson, C.J.; Collier, P.; Tea, I.; Neary, R.; Watson, J.A.; Robinson, C.; Phelan, D.; Ledwidge, M.; McDonald, K.; McCann, A.; et al. Hypoxia-induced epigenetic modifications are associated with cardiac tissue fibrosis and the development of a myofibroblast-like phenotype. *Hum. Mol. Genet.* **2014**, *23*, 2176–2188. [[CrossRef](#)]
35. Adewumi, O.; Aflatoonian, B.; Ahrlund-Richter, L.; Amit, M.; Andrews, P.W.; Beighton, G.; Bello, P.A.; Benvenisty, N.; Berry, L.S.; Bevan, S.; et al. Characterization of human embryonic stem cell lines by the International Stem Cell Initiative. *Nat Biotechnol.* **2007**, *25*, 803–816. [[CrossRef](#)]
36. Xu, Y.; Wu, F.; Tan, L.; Kong, L.; Xiong, L.; Deng, J.; Barbera, A.J.; Zheng, L.; Zhang, H.; Huang, S.; et al. Genome-wide Regulation of 5hmC, 5mC, and Gene Expression by Tet1 Hydroxylase in Mouse Embryonic Stem Cells. *Mol. Cell* **2011**, *42*, 451–464. [[CrossRef](#)]
37. Smith, Z.D.; Meissner, A. DNA methylation: Roles in mammalian development. *Nat. Rev. Genet.* **2013**, *14*, 204–220. [[CrossRef](#)]
38. Chen, C.-C.; Wang, K.-Y.; Shen, C.-K.J. The Mammalian de Novo DNA Methyltransferases DNMT3A and DNMT3B Are Also DNA 5-Hydroxymethylcytosine Dehydroxymethylases. *J. Biol. Chem.* **2012**, *287*, 33116–33121. [[CrossRef](#)]
39. Agrawal, R.; Dale, T.P.; Al-Zubaidi, M.A.; Malmgulwar, P.B.; Forsyth, N.R.; Kulshreshtha, R. Pluripotent and Multipotent Stem Cells Display Distinct Hypoxic miRNA Expression Profiles. *PLoS ONE* **2016**, *11*, e0164976. [[CrossRef](#)]
40. Rajala, K.; Vaajasaari, H.; Suuronen, R.; Hovatta, O.; Skottman, H. Effects of the physiochemical culture environment on the stemness and pluripotency of human embryonic stem cells. *Stem Cell Stud.* **2011**, *1*, 3. [[CrossRef](#)]
41. Chen, H.-F.; Kuo, H.-C.; Chen, W.; Wu, F.-C.; Yang, Y.-S.; Ho, H.-N. A reduced oxygen tension (5%) is not beneficial for maintaining human embryonic stem cells in the undifferentiated state with short splitting intervals. *Hum. Reprod.* **2009**, *24*, 71–80. [[CrossRef](#)]
42. Närvä, E.; Pursiheimo, J.-P.; Laiho, A.; Rahkonen, N.; Emani, M.R.; Viitala, M.; Laurila, K.; Sahla, R.; Lund, R.; Lähdesmäki, H.; et al. Continuous Hypoxic Culturing of Human Embryonic Stem Cells Enhances SSEA-3 and MYC Levels. *PLoS ONE* **2013**, *8*, e78847. [[CrossRef](#)]
43. Ludwig, T.E.; Levenstein, M.E.; Jones, J.M.; Berggren, W.T.; Mitchen, E.R.; Frane, J.L.; Crandall, L.J.; Daigh, C.A.; Conard, K.R.; Piekarczyk, M.S.; et al. Derivation of human embryonic stem cells in defined conditions. *Nat. Biotechnol.* **2006**, *24*, 185–187. [[CrossRef](#)] [[PubMed](#)]
44. Forsyth, N.R.; Kay, A.; Hampson, K.; Downing, A.; Talbot, R.; McWhir, J. Transcriptome alterations due to physiological normoxic (2% O₂) culture of human embryonic stem cells. *Regen. Med.* **2008**, *3*, 817–833. [[CrossRef](#)] [[PubMed](#)]
45. Westfall, S.D.; Sachdev, S.; Das, P.; Hearne, L.B.; Hannink, M.; Roberts, R.M.; Ezashi, T. Identification of Oxygen-Sensitive Transcriptional Programs in Human Embryonic Stem Cells. *Stem Cells Dev.* **2008**, *17*, 869–881. [[CrossRef](#)] [[PubMed](#)]
46. Watson, J.A.; Watson, C.J.; McCann, A.; Baugh, J. Epigenetics, the epicenter of the hypoxic response. *Epigenetics* **2010**, *5*, 293–296. [[CrossRef](#)]
47. Lees, J.G.; Cliff, T.S.; Gammilonghi, A.; Ryall, J.G.; Dalton, S.; Gardner, D.K.; Harvey, A.J. Oxygen Regulates Human Pluripotent Stem Cell Metabolic Flux. *Stem Cells Int.* **2019**, *2019*, 8195614–8195617. [[CrossRef](#)]

48. Kim, M.; Park, Y.-K.; Kang, T.-W.; Lee, S.-H.; Rhee, Y.-H.; Park, J.-L.; Kim, H.-J.; Lee, D.; Lee, D.; Kim, S.-Y.; et al. Dynamic changes in DNA methylation and hydroxymethylation when hES cells undergo differentiation toward a neuronal lineage. *Hum. Mol. Genet.* **2014**, *23*, 657–667. [[CrossRef](#)]
49. Sun, W.; Zang, L.; Shu, Q.; Li, X. From development to diseases: The role of 5hmC in brain. *Genomics* **2014**, *104*, 347–351. [[CrossRef](#)]
50. Szwagierczak, A.; Bultmann, S.; Schmidt, C.S.; Spada, F.; Leonhardt, H. Sensitive enzymatic quantification of 5-hydroxymethylcytosine in genomic DNA. *Nucleic Acids Res.* **2010**, *38*, e181. [[CrossRef](#)]
51. Tahiliani, M.; Koh, K.P.; Shen, Y.; Pastor, W.A.; Bandukwala, H.; Brudno, Y.; Agarwal, S.; Iyer, L.M.; Liu, D.R.; Aravind, L.; et al. Conversion of 5-Methylcytosine to 5-Hydroxymethylcytosine in Mammalian DNA by MLL Partner TET1. *Science* **2009**, *324*, 930–935. [[CrossRef](#)]
52. Gopalakrishnan, S.; Van Emburgh, B.O.; Robertson, K.D. DNA methylation in development and human disease. *Mutat. Res. Fundam. Mol. Mech. Mutagen.* **2008**, *647*, 30–38. [[CrossRef](#)]
53. Pelosi, E.; Forabosco, A.; Schlessinger, D. Germ cell formation from embryonic stem cells and the use of somatic cell nuclei in oocytes. *Ann. N. Y. Acad. Sci.* **2011**, *1221*, 18–26. [[CrossRef](#)]
54. Totonchi, M.; Hassani, S.-N.; Sharifi-Zarchi, A.; Tapia, N.; Adachi, K.; Arand, J.; Greber, B.; Sabour, D.; Araúzo-Bravo, M.J.; Walter, J.; et al. Blockage of the Epithelial-to-Mesenchymal Transition Is Required for Embryonic Stem Cell Derivation. *Stem Cell Rep.* **2017**, *9*, 1275–1290. [[CrossRef](#)]
55. Li, B.; Carey, M.; Workman, J.L. The Role of Chromatin during Transcription. *Cell* **2007**, *128*, 707–719. [[CrossRef](#)]
56. Li, J.-Y.; Pu, M.-T.; Hirasawa, R.; Li, B.-Z.; Huang, Y.-N.; Zeng, R.; Jing, N.-H.; Chen, T.; Li, E.; Sasaki, H.; et al. Synergistic Function of DNA Methyltransferases Dnmt3a and Dnmt3b in the Methylation of *Oct4* and *Nanog*. *Mol. Cell. Biol.* **2007**, *27*, 8748–8759. [[CrossRef](#)]
57. Zhu, C.; Yu, J.; Pan, Q.; Yang, J.; Hao, G.; Wang, Y.; Li, L.; Cao, H. Hypoxia-inducible factor-2 alpha promotes the proliferation of human placenta-derived mesenchymal stem cells through the MAPK/ERK signaling pathway. *Sci. Rep.* **2016**, *6*, 35489. [[CrossRef](#)]